

Conservation of Mass in a Piping Network

by

Samantha Rochelle Heim

A PROJECT

submitted to

Oregon State University

University Honors College

in partial fulfillment of  
the requirements for the  
degree of

Honors Baccalaureate of Science in Mechanical Engineering (Honors Associate)

Presented June 3, 2010  
Commencement June 2010



AN ABSTRACT OF THE THESIS OF

Samantha Rochelle Heim for the degree of Honors Baccalaureate of Science in Mechanical Engineering presented on June 3, 2010. Title: Conservation of Mass in a Piping Network.

Abstract approved: \_\_\_\_\_

Deborah Pence

Using returnable bottles within a brewery setting can lower costs associated with purchasing new bottles as well as reduce the energy associated with recycling glass bottles. A commercial dishwasher was retrofit specifically to wash bottles. The design and assembly of the piping flow network, testing of water flow through the network and testing of the cleanliness of the bottles post washing are presented in this study. This requires simultaneous analyses of mass and energy conservation equations.

The flow out of the piping network was examined by running water through the network and collecting the exiting water in beakers for a specified period of time. These data were used to determine the exiting velocity and report the variations in nozzle mass flow rate. The measured exit velocity of water was found to vary from nozzle to nozzle by as much as 11%. All measured velocities were within 5.7% of those predicted from theory. The outer nozzles had a lower velocity than the nozzles closer to the water source. Although the velocity was different than the calculated values, the total mass exiting the piping network was equal to within  $\pm 0.25\%$  of the calculated value. The bottles were swabbed to determine compliance with food safety standards. All cleaned bottles met food safety standards.

Key Words: piping, conservation, mass, pressure, loss

Corresponding e-mail address: [heims@onid.orst.edu](mailto:heims@onid.orst.edu)

Conservation of Mass in a Piping Network

by

Samantha Rochelle Heim

A PROJECT

submitted to

Oregon State University

University Honors College

in partial fulfillment of  
the requirements for the  
degree of

Honors Baccalaureate of Science in Mechanical Engineering (Honors Associate)

Presented June 3, 2010  
Commencement June 2010

Honors Baccalaureate of Science in Mechanical Engineering project of Samantha Rochelle Heim presented on June 3, 2010.

APPROVED:

---

Mentor, representing Mechanical Engineering

---

Committee Member, representing Mechanical Engineering

---

Committee Member, representing Mechanical Engineering

---

Dean, University Honors College

I understand that my project will become part of the permanent collection of Oregon State University, University Honors College. My signature below authorizes release of my project to any reader upon request.

---

Samantha Rochelle Heim, Author

## **ACKNOWLEDGMENTS**

I would like to thank my mentor, Dr. Deborah Pence, for her time and effort in helping me through this process. Without her patience, this project would not have been possible. I would also like to thank Carolyn Beaudry and Sean Hunter for their contributions to the project of the retrofitted commercial dishwasher on which this project is based.

# TABLE OF CONTENTS

	<u>Page</u>
CHAPTER 1: INTRODUCTION.....	1
CHAPTER 2: BACKGROUND.....	2
CHAPTER 3: DESIGN.....	4
3.1: Design Concept.....	4
3.2: Design Analysis.....	7
Conservation of mass.....	7
Conservation of energy.....	10
3.3: Piping Network Analysis.....	15
CHAPTER 4: PIPING NETWORK ASSEMBLY.....	17
CHAPTER 5: TESTING.....	18
5.1: Mass Flow Rate Calculations .....	18
5.2: Mass Flow Testing Procedure.....	18
5.3: Cleanliness Inspection.....	21
CHAPTER 6: RESULTS.....	23
CHAPTER 7: CONCLUSION.....	28
BIBLIOGRAPHY.....	29
APPENDICES.....	30
APPENDIX A: NOZZLE CATALOG.....	31
APPENDIX B: PIPING NETWORK PART SUMMARY.....	32
APPENDIX C: NOMENCLATURE.....	33
APPENDIX D: PIPING NETWORK CALCULATIONS.....	34
APPENDIX E: VARIABLE VALUES.....	36

## LIST OF FIGURES

Figure	Page
1. Complete piping network with components labeled.....	5
2. Resistance analogy in half of the piping network with pressure nodes, pipe sections and nozzles.....	8
3. Fluid flow through the cross.....	13
4. Complete piping network with the numbered nozzles corresponding to the beakers.....	19
5. Setup of the beakers for catching the water exiting the nozzles of the piping network.....	20
6. Complete configuration of bottles in the retrofitted commercial dishwasher.....	22
7. Average experimental and theoretical outgoing velocity per nozzle (graphical representation of Table 9).....	25
8. Total outgoing mass from the piping network for 5 Seconds (graphical representation of Table 10).....	27



## LIST OF TABLES

Table	Page
1. Values for the diameter of each pipe segment and exit diameter of nozzles.....	8
2. Values for the length of each pipe segment and nozzle.....	9
3. Equations for the conservation of mass for the control volumes at the nozzle junctions.....	10
4. Conservation of energy equations for the pipe sections and nozzles in piping network.....	13
5. Velocity and minor loss coefficient for piping configurations (Fried & Idelchik, 1989) .....	14
6. Minor head loss components for the piping network .....	15
7. Exit velocity for each individual nozzle .....	16
8. Mass flow rates per nozzle in kg/s .....	24
9. Velocity per nozzle in m/s.....	24
10. Mass exiting each nozzle and total mass exiting for 5 seconds in kg.....	26
11. SpotCheck test results.....	27

## LIST OF APPENDICES

Appendix	Page
A. NOZZLE CATALOG .....	31
B. PIPING NETWORK PART SUMMARY .....	32
C. NOMENCLATURE .....	33
D. PIPING NETWORK CALCULATIONS.....	34
E. VARIABLE VALUES.....	36

## LIST OF APPENDIX TABLES

Table	Page
B1. Material and quantity of the piping network parts.....	32
C1. Nomenclature used throughout equations .....	33
E1. Reynolds numbers for individual pipe sections.....	36
E2. Friction factor values for individual pipe sections.....	36
E3. Frictional head loss values for individual pipe sections.....	36
E4. Minor head loss values for individual pipe sections .....	36

## CHAPTER 1: INTRODUCTION

In an effort to reduce energy needs associated with bottle recycling and costs associated with the purchase of new bottles, a local brewery is interested in re-using bottles. To avoid issues of solid waste accumulation in previous bottle washing efforts (Mata & Costa, 2001), the brewery proposes use of special screen-printed labels on the bottles that can withstand a minimum of 15 wash cycles (SSTC Services Du Premier Ministre, 2000).

An existing dishwashing machine was retrofit specifically for washing bottles. The present study involves the design of a symmetric pipe flow network to replace the bottom rotating spray arm in the existing dishwasher. The piping network was designed to uniformly distribute water for purposes of simultaneously cleaning 16 bottles. Following assembly of the flow network, it was tested for flow uniformity prior to being installed in the dishwasher. Once in place, the modified dishwasher was tested to determine its cleaning capability.

Design of the pipe flow network required simultaneous analyses of mass and energy conservation equations. Fabrication of the piping network required consideration of material-material as well as material-fluid compatibility, where the dishwashing fluid includes harsh chemicals including sodium meta-silicate (Gideon, personal communication, January 26, 2010). Testing of pure water flow through the piping network included (1) a catch and weigh analysis to assess the uniformity of flow distribution through the 16 nozzles as well as that of the velocity of water exiting each nozzle, and (2) the ability for the flow network to adequately clean the bottles (Heim, Beaudry & Hunter, 2010).

## CHAPTER 2: BACKGROUND

A bottle washer is a mandatory component of a returnable bottle program. The program involves the customer returning empty bottles when they return to purchase more beer. The returned bottles would be washed in the bottle washer in preparation for refilling. In principle, this program eliminates the amount of bottles being recycled and/or thrown away. Returnable bottles would typically be part of a small scale process, accounting for anywhere up to 20% of the total glass bottles distributed. There are many benefits for this process. The main benefit of implementing a returnable bottle program is a smaller environmental impact than occurs when using non-reusable bottles. A study was done in 2001 analyzing the environmental impact as a function of the percentage of beer bottles reused. When less than half the total glass bottles are reusable, the reusable bottles have a lower impact than non-reusable bottles in all categories of environmental impact. This includes the effect on global warming and final solid waste. Brewing beer contributes to global warming. Carbon dioxide is the main component of emissions that contribute to global warming (Mata & Costa, 2001). Carbon dioxide is produced during the fermentation process and is also used for carbonating the beer. Carbon dioxide is also commonly used to flush bottles, cans and kegs before they are filled. When using a bottle washer, the need for carbon dioxide is less than when flushing the bottles since the bottles have already gone through a sterilization process. Also, in a study done in Japan, they found that if a person switched from drinking 500 milliliters of beer from a can to drinking the same amount from a returnable bottle, the carbon dioxide emissions would be reduced by approximately 130 grams due to the decrease of carbon dioxide used to flush the cans. In the same study, they found that if all the beverage containers were

changed from cans and paper containers to returnable bottles, the carbon dioxide emissions would be reduced by about 57%. In addition, there would be about 1.25 million tons less of solid waste (Edahiro, 2004). The amount of solid waste sent to landfills or water treatment facilities is also decreased by the use of reusable bottles. Solid waste includes scrap metal, oil and waste from the treatment plant. It also includes any solid waste from the brewery such as broken glass bottles and packaging material. The use of a bottle washer would reduce the use of packaging material as the bottles would be returned, hence new bottles would not be needed. Also no longer needed would be the pallets and plastic wrapping in which the bottles come. While the amount of broken bottles may increase due to the bottle weakening after multiple uses, it does not account for a large portion of waste.

Another way the bottle return process has the potential to better the environment is by decreasing the amount of litter. For example, Gilson (2010) estimated that if the United States switched entirely to a returnable bottle system, the amount of litter on the highway could be reduced by 11.3%. Gilson proposed that if the reusable bottles had a sufficiently high deposit placed on them, this would serve as an incentive for the customers to return the bottles. The result would be an increase in the number of bottles returned, therefore a decrease in the number of bottles littering the streets and highways. Therefore, it is possible that along with a bottle return program, the retrofit of an existing dishwasher could be a plus to the environment, both by slowing down global warming and also making the roads more beautiful.

## CHAPTER 3: DESIGN

There are many individuals who brew beer, either privately or commercially on a small-scale. There are many small breweries that do not currently bottle their beer, rather sell it only in pressurized vessels. The ability of small-scale brewers to bottle their beer bottles may allow them to expand their business. Furthermore, implementing an environmentally conscientious bottle reuse program provides the additional benefit of a marketing angle for these small brewers. A simple retrofit of a commercial dishwasher will provide these brewers with an inexpensive, efficient method of preparing their bottles for the filling process (Heim, Beaudry & Hunter, 2010). The major component of the retrofit of the dishwasher is the piping network. Design constraints required that 1) the retrofit washer would clean 16 bottles simultaneously, 2) each bottle had an individual nozzle that would deliver water into it during the washing process, 3) that each nozzle must deliver the same spray (velocity and shape), and 4) the entire retrofit be as cost effective as possible. The flow uniformity was determined to be best achieved using flow symmetry and high resistance nozzles. The cost could be minimized by using commercially available components.

For the present situation, there were limited resources to weld the pipes together; therefore, all of the parts had to be threaded. This allowed for a quick assembly time and allowed for all tolerances to be met.

### 3.1: Design Concept

A solid model of the final piping network design can be seen in Figure 1.

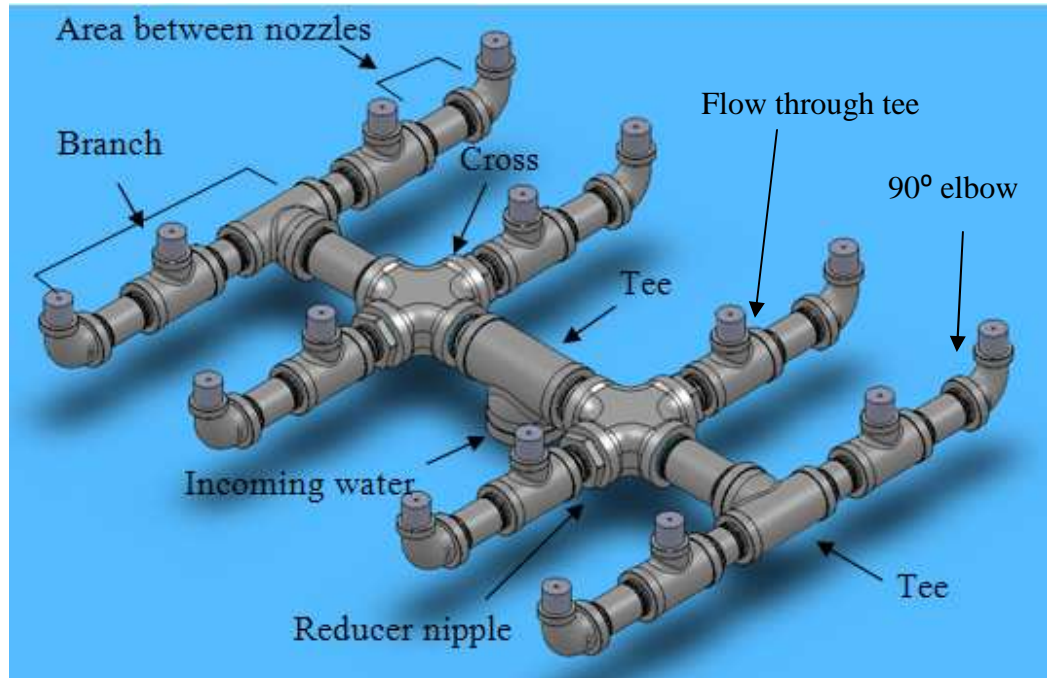


**Figure 1: Complete piping network with components labeled.**

Water flows from the bottom of the network, as noted by incoming water in Figure 1, and splits equally, in the tee. Looking at one side of this split flow, the water flows through a cross such that approximately half the water flows to the outer most branches and approximately one-quarter of the water flows out of each of the remaining branches connected to the cross. The water that flows to the outer branches splits equally between these two branches. In each branch, approximately half of the water exits through the inner nozzle and the remaining water flows out of the outer nozzle.

Restricted to standardized parts, the pipe network was not able to be fully optimized in terms of pipe diameter for the current application. The material used for the crosses, tees and elbows is galvanized malleable iron. The material was chosen because of its high strength as well as inexpensive cost. Galvanized iron has a harder finish than the standard black finish and will ensure that the iron will not be damaged by the



chemicals or high temperature water of the dishwasher (Callister, 2007). The pipe reducer nipples, of which there are four, are made of schedule 40 steel. These are the connectors between the cross and the side branches, as noted in Figure 1. They scale down the inner diameter of the cross to the final diameter of the pipe segments in the side branches. This material was chosen because of the inexpensive cost and its strength is adequate for the given application. Schedule 40 steel is compatible with malleable iron and will not produce a destructive reaction. The nozzles were made of stainless steel which is also compatible with malleable iron threads. The steel was chosen because of its resistance to corrosion. The detergent includes sodium metasilicate, which cleans the bottles by attaching to larger molecules and dragging them out through the water (Material Safety Data Sheet). Luckily this detergent does not corrode any of the specified materials because it has an anticorrosive property. However, it may leave deposits on stainless steel when used with water above a temperature of 158°F.

The basic engineering design principle behind the piping design is one with a high degree of symmetry and with the nozzles having the largest resistance to flow. This should ensure that the water will be approximately equal through each nozzle. Data provided by the nozzle manufacturer specifies the mass flow rate as a function of supply pressure. This makes it possible to calculate a loss coefficient for the nozzles. The configuration of the piping network has minimum twists and turns in an effort to minimize minor losses everywhere but at the nozzles. In addition, the flow will experience frictional losses through each segment of the piping network. The pressure loss through the flow network can be modeled as resistors, similar to resistors in an electrical network. Figure 2 illustrates the resistances within the flow network. Also

noted in Figure 2 are pressure nodes denoted by dots and labeled by letters and pipe segments and nozzle segments denoted by numbers. The numbers are associated with velocities through these segments. Diameter and length specifications for each segment are provided in Tables 1 and 2, respectively.

### **3.2: Design Analysis**

With knowledge of the pressure of the water supplied to the flow network, an analysis conducted with the conservation of mass and conservation of energy equations allows for the assessment of velocity from, and mass flow rate through, each nozzle. For this case, the fluid being used is water. The density and viscosity of water used in the present analyses are  $983 \text{ kg/m}^3$  and  $0.000467 \text{ N}\cdot\text{s/m}^2$ , respectively. The static pressure at the location where the piping network was to be connected was measured using Water Source M1002-4L water pressure gauge and found to be 240 kPa.

#### **Conservation of mass.**

Applying the conservation of mass equations to the flow network requires analysis of ten control volumes. These consist of one control volume at the cross, one control volume at the tee and one control volume at the base of each of the eight nozzles (i.e. either a  $90^\circ$  elbow or a flow through tee). Control volumes at the cross, the tee, a flow through tee and a  $90^\circ$  elbow are shown as dashed lines for Figure 2. A control volume shown for the pipe segment between pressure nodes H and J is a typical control volume for an energy balance.

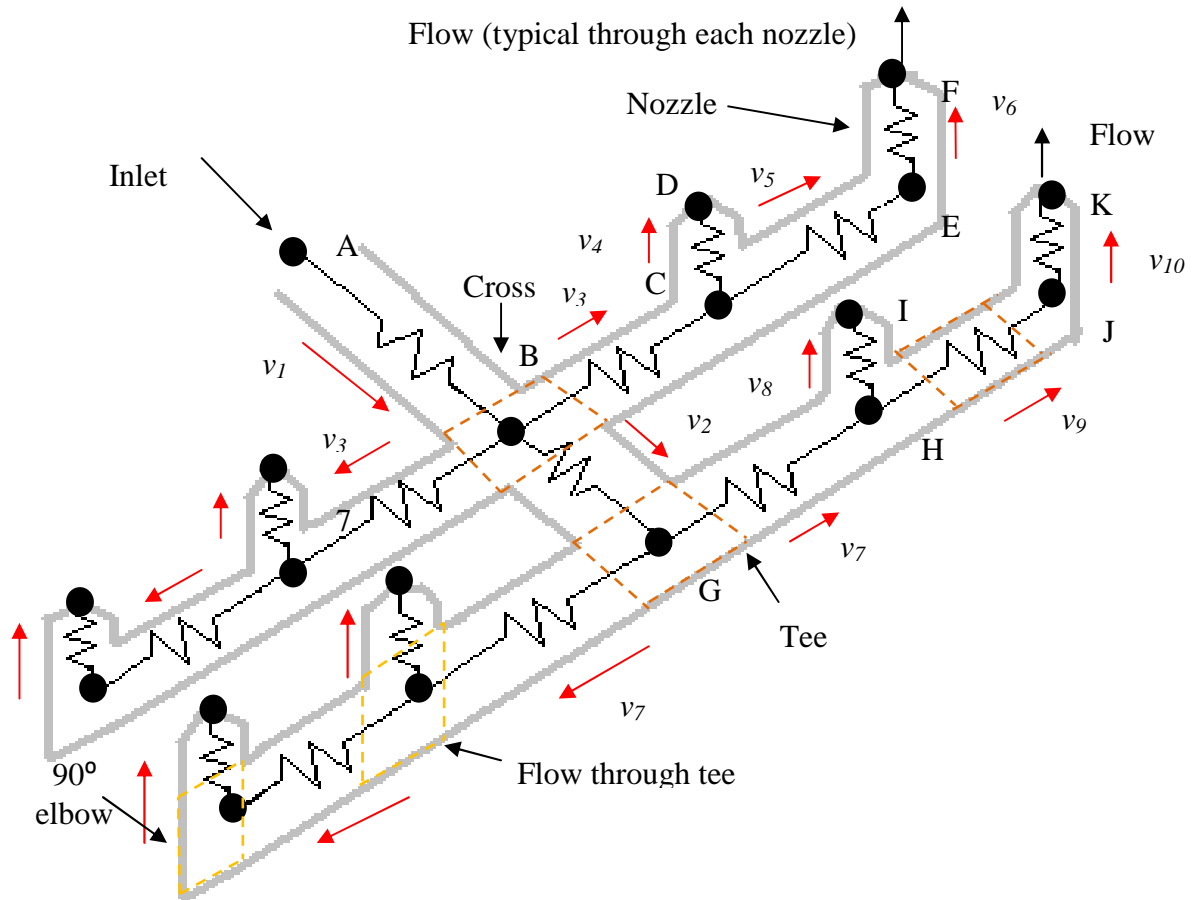


Figure 2: Resistance analogy in half of the piping network with pressure nodes, pipe sections and nozzles

Table 1: Values for the diameter of each pipe segment and exit diameter of nozzles

Component	Diameter (cm)
Pipe Sections	
$d_1$ (A to B)	1.905
$d_2$ (B to G)	1.905
$d_3$ (B to C)	1.27
$d_5$ (C to E)	1.27
$d_7$ (G to H)	1.27
$d_9$ (H to J)	1.27
Nozzles	
$d_4$ (C to D)	0.218
$d_6$ (E to F)	0.218
$d_8$ (H to I)	0.218
$d_{10}$ (J to K)	0.218

**Table 2: Values for the length of each pipe segment and nozzle**

Component	Length (cm)
Pipe Sections	
L <sub>1</sub> (A to B)	6.35
L <sub>2</sub> (B to G)	7.62
L <sub>3</sub> (B to C)	6.35
L <sub>5</sub> (C to E)	7.62
L <sub>7</sub> (G to H)	6.35
L <sub>9</sub> (H to J)	7.62
Nozzles	
L <sub>4</sub> (C to D)	2.38
L <sub>6</sub> (E to F)	2.38
L <sub>8</sub> (H to I)	2.38
L <sub>10</sub> (J to K)	2.38

The general form of the conservation of mass equation is:

$$\frac{dm}{dt} = \sum \dot{m}_o - \sum \dot{m}_i \quad (1)$$

which is applicable for multiple flows into and out of the control volume. Because the flow is steady state, i.e. independent of time, the time rate of change of mass within the control volume will be equal to zero and equation (1) reduces to:

$$\sum \dot{m}_i = \sum \dot{m}_o \quad (2)$$

where mass flow rate,  $\dot{m}$ , is defined as:

$$\dot{m} = \rho Av \quad (3)$$

where  $\rho$  is the fluid density,  $A$  is the cross-sectional flow area and  $v$  is the velocity. The velocities in the piping network are shown as red arrows in Figure 2. Due to symmetry, only half the flow network in Figure 2 needs to be considered in the analysis. For the cross centered at node B, note that flow splits equally at 90° from the incoming flow, as can be seen from  $v_3$  on either side of the tee. Substituting  $\pi \left(\frac{d}{2}\right)^2$  for  $A$  in equation (3) and substituting equation (3) into equation (2), the conservation of mass for the control volume at the cross reduces to:

$$d_1^2 v_1 = 2d_3^2 v_3 + d_2^2 v_2 \quad (4)$$

where  $d$  is the inner diameter of the pipes intersecting the function. Similar to the cross, the tee has one incoming flow and two outgoing flows. The equation for the conservation of mass for the control volume at the tee is:

$$d_2^2 v_2 = 2d_7^2 v_7 \quad (5)$$

The cross and the tee are examples of components that have multiple exiting flows. The first nozzle junction of a branch has one inlet and two outlets while the second nozzle junction in the branch has one inlet and one outlet. The conservation equations governing mass flow for each of the control volumes at the nozzle junctions are provided in Table 3. Unknown in each of these equations is the flow velocity, for which conservation of energy analyses are needed.

**Table 3: Equations for the conservation of mass for the control volumes at the nozzle junctions**

Nozzle Junction	Equation
C	$d_3^2 v_3 = d_4^2 v_4 + d_5^2 v_5$
E	$d_5^2 v_5 = d_6^2 v_6$
H	$d_7^2 v_7 = d_8^2 v_8 + d_9^2 v_9$
J	$d_9^2 v_9 = d_{10}^2 v_{10}$

### **Conservation of energy.**

Similar to the conservation of mass, the conservation of energy can be applied to each applicable control volume. For conservation of energy analyses, ten control volumes are considered. The ten control volumes considered for conservation of energy analyses are the pipe sections and the nozzles. The steady-state head form of the conservation of energy equation, which accounts for minor losses and frictional head loss, is used to compute the velocity through each segment:

$$\frac{P_{in}}{\gamma} + \frac{v_{in}^2}{2g} + z_1 = \frac{P_{out}}{\gamma} + \frac{v_{out}^2}{2g} + z_2 + h_f + \sum h_m \quad (6)$$

In equation (6),  $z$  is the elevation relative to some reference datum,  $\gamma$  is the specific gravity (i.e. density of the fluid multiplied by the acceleration due to gravity),  $h_f$  is the frictional head loss, and  $\sum h_m$  is the sum of the minor head losses. A representative control volume is shown in Figure 2 between pressure nodes H and J, where pressure nodes are identified with a large black dot and a letter. Because the piping network has a horizontal orientation, the change in elevation is equal to zero. For convenience the equation is simplified and rearranged to:

$$P_{in} - P_{out} = \frac{1}{2}\rho(v_{out}^2 - v_{in}^2) + (h_f + \sum h_m)\rho g \quad (7)$$

Because the diameters of the pipe segments are constant across a control volume, as is the density of the fluid, the fluid velocity must also be constant. Equation (7) can now be simplified to:

$$P_{in} - P_{out} = (h_f + \sum h_m)\rho g \quad (8)$$

for pipe segments.

The effects of friction, known as frictional head loss, occur in all fluid flows, are a result of the irreversible conversion of mechanical energy to thermal energy (Kaminski & Jensen, 2005). The frictional head loss is dependent on the length and diameter of the pipe, and on the velocity of the flow according to:

$$h_f = f \frac{L}{d} * \frac{v^2}{2g} \quad (9)$$

where  $f$  is the friction factor (White 2008). The friction factor depends on the Reynolds number,  $Re$ , which is the ratio between inertia and viscous forces. The Reynolds number

is used to determine whether the flow through the pipes is laminar or turbulent. The Reynolds number is defined by:

$$Re = \frac{vd\rho}{\mu} \quad (10)$$

where  $\mu$  is the viscosity of the fluid. Laminar flow is considered smooth flow. The fluid in a laminar flow moves orderly and parallel to the pipe walls. If the Reynolds number is below 2300, the flow is assumed to be laminar. Turbulent flow undergoes mixing and fluctuations in the direction of the flow. If the Reynolds number is over 4000, the flow is considered turbulent. If the Reynolds number is between 2300 and 4000, the flow is in transition, a region or condition that is less predictable.

For laminar flow in a pipe with a circular cross section, the friction factor decreases inversely with the Reynolds number, according to:

$$f = \frac{64}{Re} \quad (11)$$

If the flow is turbulent, the friction factor is determined from:

$$\frac{1}{\sqrt{f}} = -1.8 \log \left( \left( \frac{\varepsilon/d}{3.7} \right)^{1.11} + \frac{6.9}{Re} \right) \quad (12)$$

where  $\varepsilon$  is the roughness value. For cast iron,  $\varepsilon$  is 0.26 mm  $\pm$  50% (White, 2008).

The minor head loss,  $h_m$ , accounts for losses associated with the tees, crosses and elbows in the piping network, and is a function of velocity and the minor loss coefficient,  $\zeta$ , according to

$$h_{minor} = \frac{\zeta v^2}{2g} \quad (13)$$

Empirical values of minor loss coefficients are reported for multiple piping component configurations (White 2008). Minor head losses,  $h_m$ , depend upon the inlet and exit conditions, which vary for the different components: tee, cross, through tee, and elbow.

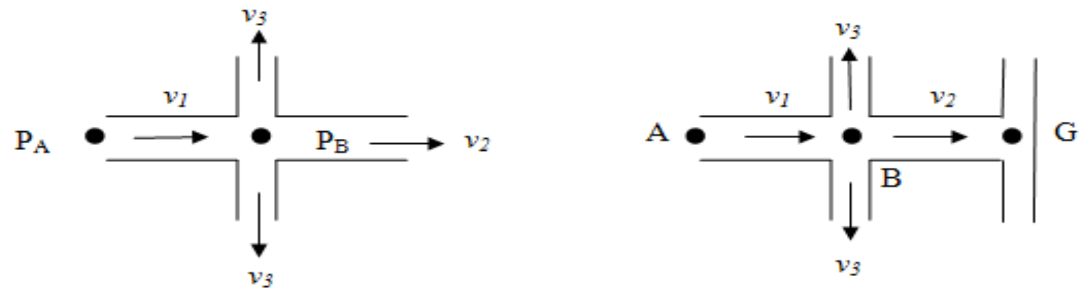


Figure 3: Fluid flow through the cross

The minor loss at the cross centered about B is influenced by how fluid enters and leaves the junction, as can be seen from Figure 3. In principle, the minor loss at the inlet of the cross at junction B should be included in the energy equation for the pipe section between nodes A and B. Likewise, the minor loss at the exit of the cross at B (in the direction of flow from B to G, noted in Figure 3b) should be included in the energy equation for the pipe section between nodes B and G. However, given the anticipated high flow resistance in the nozzle, accounting for all of the minor losses in the upstream energy balance (A to B) should not significantly alter the predicted pressure at each node. The set of conservation of energy equations for the piping network shown in Figure 2 are provided in Table 4, where  $h_{mB}$  is the minor head loss at node B.

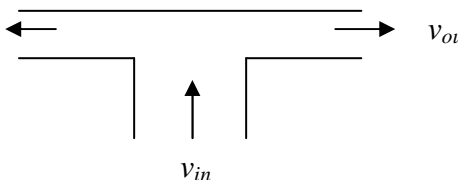
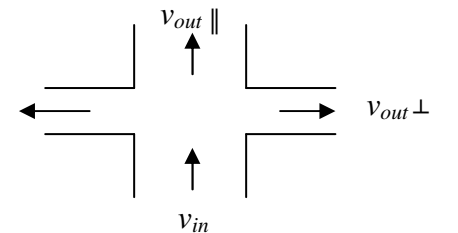
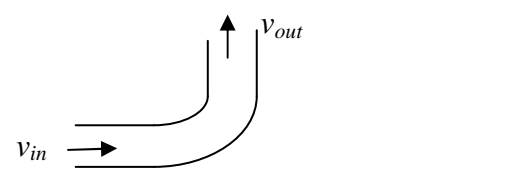
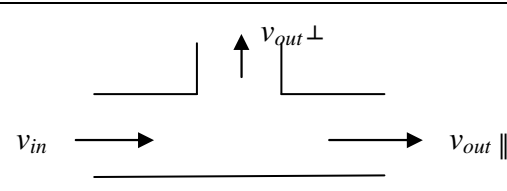
Table 4: Conservation of energy equations for the pipe sections and nozzles in piping network

Pipe Segment	Equation
Between A and B	$P_A - P_B = (h_{f1} + h_{mA} + h_{mB})\rho g$
Between B and C	$P_B - P_C = (h_{f3} + h_{mC})\rho g$
Between C and E	$P_C - P_E = (h_{f5} + h_{mE})\rho g$
Between B and G	$P_B - P_G = (h_{f2} + h_{mG})\rho g$
Between G and H	$P_G - P_H = (h_{f7} + h_{mH})\rho g$
Between H and J	$P_H - P_J = (h_{f9} + h_{mJ})\rho g$
Nozzle	
Between C and D	$P_C - P_D = (h_{mD})\rho g$
Between E and F	$P_E - P_F = (h_{mF})\rho g$
Between H and I	$P_H - P_I = (h_{mI})\rho g$
Between J and K	$P_J - P_K = (h_{mK})\rho g$



The minor loss coefficient and velocity used in assessing a minor loss values for each type of component in the present study are noted in Table 5. For the present work, a numerical value of the minor loss coefficient,  $\zeta$ , and the velocity,  $v$ , used to compute each minor loss are tabulated in Table 6.

**Table 5: Velocity and minor loss coefficient for piping configurations (Fried & Idelchik, 1989)**

Configuration	Component
	Tee $\zeta = 2$ $v = v_{in}$
	Cross $\zeta = 2$ $v = v_{in}$
	90° Bend $\zeta = 1$ $v = v_{in} = v_{out}$
	Flow Through Tee $\zeta = 2$ $v = v_{in}$

An empirical value for the loss coefficient of the nozzles is not known. Rather a table of flow rate versus nozzle supply pressure is provided by the nozzle manufacturer. Given a measured static inlet pressure of 240 kPa (35 psi), the corresponding nozzle flow rate for

a part #SSM202 (Appendix A) as specified to be 0.0001 m/s (1.7 gal/min). For a known nozzle exit area of 0.002 m<sup>2</sup>, the velocity can be determined from the flow rate using:

$$v = \frac{\dot{V}}{A} \quad (14)$$

Using these values of velocity and pressure drop, the loss coefficient can be determined using:

$$\zeta = \frac{\Delta P}{\frac{1}{2}\rho v^2} \quad (15)$$

Note that the exit area was determined from the exit diameter of the nozzle, which was measured with calipers to be 2.2 +/- 0.005mm.

**Table 6: Minor head loss components for the piping network**

Minor head loss	Velocity	Minor loss coefficient ( $\zeta$ )	Component
$h_{mA}$	$v_1$	2	Tee
$h_{mB}$	$v_1$	2	Cross
$h_{mC}$	$v_3$	2	Tee with continuing flow
$h_{mD}$	$v_4$	0.5	Nozzle
$h_{mE}$	$v_5$	1	Elbow
$h_{mF}$	$v_6$	0.5	Nozzle
$h_{mG}$	$v_2$	2	Tee
$h_{mH}$	$v_7$	2	Tee with continuing flow
$h_{mI}$	$v_8$	0.5	Nozzle
$h_{mJ}$	$v_9$	1	Elbow
$h_{mK}$	$v_{10}$	0.5	Nozzle

### 3.3: Piping Network Analysis

The goal of the piping network is to have a uniform velocity of water exiting each nozzle. Designing the network with a high degree of symmetry and with nozzles having high flow resistance provides flow discharging from nozzles to be fairly uniform.

Although an estimate of nozzle velocity was made to assess the loss coefficient in the

nozzles, the velocities through each segment and the exit velocity from each nozzle is calculated using the conservation equations provided in Table 4, conservation of mass equations in Table 3, flow network dimensions in Tables 1 and 2, and with knowledge of a specified mass flow rate entering the piping network. The exit velocities are provided in Table 7. For the present case, the mass flow rate into the piping network is 1.46 kg/s.

The set of equations for the conservation of mass and the conservation of energy were written as a series of equations in Engineering Equation Solver (EES<sup>®</sup>), a simultaneous equation solver. The EES code is provided in Appendix D. Note that the Reynolds numbers were checked to confirm the assumption of turbulent flow. The Reynolds numbers, determined by equation (10), through each pipe section are provided in Table 7. Using equation (12), the turbulent friction factor through each pipe section is tabulated in Table 8. Using equation (9), the frictional head loss through each pipe section is tabulated in Table 9. Using equation (13) and the values from Table 6, the minor head loss through each pipe section is tabulated in Table 10. All tables are located in Appendix E.

**Table 7: Exit velocity for each individual nozzle.**

Nozzle	Exiting velocity (m/s)
4	30.02
6	30.03
8	29.84
10	28.62

#### **CHAPTER 4: PIPING NETWORK ASSEMBLY**

Because the piping assembly is made of standardized parts, the assembly was straight forward. It was necessary that when assembling the parts, the assembly started with the outer most nozzles, working backwards to the flow inlet (Heim, Beaudry & Hunter, 2010). With standardized parts, it can be difficult to get the parts to thread the same distance. This is easier to control when starting from the outside. The branches are the only ones that are directionally limited in that they all have to face the same direction; upward. The assembly of the network was accomplished with a pipe wrench so as to get the largest force to secure the pipes. The manufacturers specify a distance in which the pipes should be threaded, but this can vary due to tolerances in the materials. The actual distance between nozzles and between pipes were measured with a set of calipers, with an uncertainty of  $\pm 0.1$  mm. A summary of the parts used can be found in Appendix B.

## CHAPTER 5: TESTING

The reasoning behind testing the piping network is to determine if there is uniform flow exiting the nozzles and if the flow, as delivered, sufficiently cleans the bottles. The testing proceeded in two stages. First, the mass flow rate through each nozzle was determined using a catch and weigh technique. These values, as well as the exit velocities, were studied for uniformity between the nozzles. Second, ensuring uniform flow rates, three bottles were tested for cleanliness. Calculations presented predict a minimal difference between the velocities of water exiting the nozzles resulting in approximately equal flow within  $\pm 0.1\%$  difference as shown in Table 7.

### 5.1: Mass Flow Rate Calculations

The catch and weigh technique was used to find the mass flow rate from each nozzle. The mass flow rate is calculated by

$$\dot{m} = \frac{\Delta m}{\Delta t} \quad (16)$$

where  $\Delta m$  is the mass collected over a time interval  $\Delta t$ . Water exiting each nozzle is caught in beakers. Each beaker is weighed prior to and after the accumulation of water. The difference is used to assess the mass. The exiting velocities can be found from the mass flow rate through each nozzle.

$$v = \frac{\dot{m}}{\rho \pi \frac{d^2}{4}} \quad (17)$$

### 5.2: Mass Flow Testing Procedure

For testing purposes, the piping network was setup with a pump and water hose at the entrance of the piping network. The pressure for the incoming water was given by the pump specifications and checked with a Water Source M1002-4L water pressure gauge,

which has an uncertainty of  $\pm 6.895$  kPa. The water entered the piping network at a pressure of 241.3 kPa.



**Figure 4: Complete piping network with the numbered nozzles corresponding to the beakers**

During a test, water from eight nozzles was simultaneously caught. The nozzles tested are those labeled in Figure 4. As shown in Figure 5, eight beakers were arranged on the ground, spaced similarly to that of the nozzles. Each beaker was labeled with a number corresponding to that on the nozzle. The data were only collected for one side at a time due to the symmetry of the piping network. The nozzles labeled in Figure 4 were tested initially, followed by a repeat of a test using the other eight nozzles.

The piping network was held with the nozzles pointing downwards so the water could be easily directed into the beakers. The water was turned on and let run for a specified amount of time through the piping network before moving the piping network and nozzles over the beakers. This was done to assure that the flow is steady throughout

the network before collecting data. Once the nozzles were each placed over their corresponding beaker, the stopwatch, with a resolution of  $\pm 0.01$  seconds, was started. After five seconds passed, the flow stream from the piping network was removed from the location of the beakers and the timer stopped.

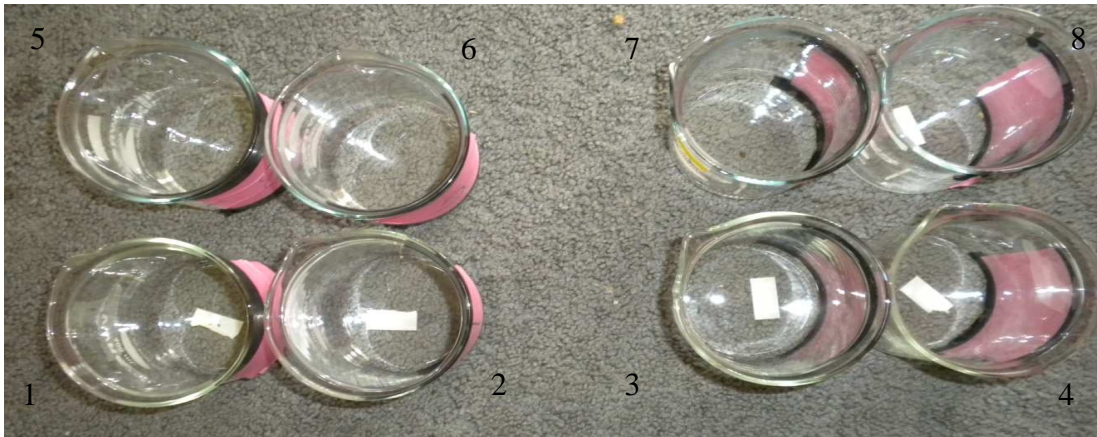


**Figure 5: Setup of the beakers for catching the water exiting the nozzles of the piping network**

The beakers before and after water collection were then weighed on a Mettler PM11, with a resolution of  $\pm 0.01$  grams. The uncertainty in measuring the mass was assessed by moving the nozzles quickly over the beakers. The beakers were weighed before to find this contribution to uncertainty in the mass measurement which was determined to be 3 g. The total uncertainty in the mass flow rate measurements were calculated using the Kline and McClintok method (Figliola & Beasley). The uncertainty in the mass flow is calculated by

$$\pm \dot{m} = \left[ \left( \frac{1}{t} \right)^2 u_t^2 + \left( -\frac{m}{t^2} \right)^2 u_m^2 \right]^{\frac{1}{2}} \quad (18)$$

where  $u_t$  is the uncertainty of the measurement of time and  $u_m$  is the total uncertainty of the mass measurement based on the resolution of the scale and uncertainty in measuring the mass. The total uncertainty of the mass measurement is calculated by:

$$u_m = \sqrt{u_{m_{resolution}}^2 + u_{m_{measuring}}^2} \quad (19)$$

### 5.3: Cleanliness Inspection

Sixteen 22 ounce bottles were filled with a sugary fluid and let sit for 24 hours. A sugary fluid was used to give a clear coat of glucose in, and around, the bottle. Glucose exists in the majority of foods and by using a sugary fluid, it will easy to determine if any remains after the dishwasher run. Once 24 hours passed, the fluid was poured out of the bottles and the bottles were placed in the retrofitted commercial dishwasher, as shown in Figure 6. Note the rack was designed as part of the retrofit of a commercial dishwasher. For more information reference Heim, Beaudry & Hunter (2010). The bottles were put through a standard dishwasher run which consists of three cycles: detergent, sanitizing and rinse. One run lasts approximately 90 seconds.

Once the run was finished, three bottles were tested for cleanliness. The bottles were chosen from different locations in the bottle rack to ensure that bottles in each section will be cleaned. The bottles above nozzles one, three and eight were selected. The cleanliness was determined by using SpotCheck<sup>®</sup>, which determines the existence of glucose and is used as a food safety check.

Three separate locations on a bottle, the bottom of the inside, inside the neck and on the mouth, were independently swabbed. These three locations were chosen as they are expected to have the largest possible source of residue. The swab test will indicate whether or not there is sufficient flow and velocity from the nozzle to clean the bottom of the bottle and rinse out the entire inside of the bottle. The inside of the neck was tested because this small slope in the bottle may contain trapped residue if the spray angle of the nozzle is not great enough at this location. The mouth of the bottle is the location of the



greatest amount of saliva. There are valleys for the saliva to catch, all of which must be cleaned. For a bottle to be reusable, the bottle will have to pass a food safety test.

After each location on the bottle was swabbed, the swab was placed in the provided enclosure. A reagent is then placed into the enclosure and allowed to sit for three minutes. If after the three minutes the solution changes color from clear to green, the swab tests positive for glucose. If the solution stays clear, the location tests negative for glucose and is considered clean by food safety standards (Hygiena).



**Figure 6: Complete configuration of bottles in the retrofitted commercial dishwasher.**

## CHAPTER 6: RESULTS

There were a total of four tests conducted to gather data on the mass output of the piping network. The mass flow rates were calculated and the average was taken for each nozzle as shown in Table 8. Also reported in the table are the standard deviation measurements as well as the mass flow rates predicted by theory. The standard deviation for the runs was assessed using:

$$\sigma = \sqrt{\frac{\sum(x-\bar{x})^2}{N}} \quad (20)$$

where  $x$  is the value for each run,  $\bar{x}$  is the average value and  $N$  is the number of tests conducted. The experimental uncertainty in mass flow measurements is 0.01 kg/s.

Evident from Table 8 is that the mass flow rate varied between nozzles by as much as 11% and differed from that predicted by theory by as much as 5.7%. Flow from nozzles 1-4 is below the predicted values whereas flow from nozzles 5-8 are above predicted values. It makes sense that flow through nozzles 5-8 are higher than through nozzles 1-4 because the inlet pressure is expected to be higher for nozzles 5-8 due to a lower path of resistance from the inlet. Although flow through nozzles 1 & 4, 2 & 3, 6 & 7, and 5 & 8 are not equal, as anticipated due to symmetry, they vary by no more than 2%. These differences are higher than those expected from experimental uncertainty, but can be expected given variations in assembly and mass flow rate of the shelf components.

Experimental values of velocities exiting each nozzle per test conducted as well as the averaged values are tabulated in Table 9. The average experimental velocity from the nozzles varies from the theoretical value by as much as 2.93 m/s.

**Table 8: Mass flow rates per nozzle in kg/s**

Nozzle	Test				Average	$\sigma$	Theoretical	% difference
	1	2	3	4				
1	9.94	10.57	9.87	11.18	10.39	0.61	11.01	5.63
2	9.87	10.52	10.49	11.8	10.67	0.81	11.00	3.00
3	9.84	10.81	10.78	10.97	10.6	0.51	11.00	3.64
4	9.77	10.81	11.12	10.63	10.58	0.57	11.01	3.91
5	10.7	11.8	11.34	12	11.46	0.58	11.07	3.52
6	10.77	11.7	11.4	11.86	11.43	0.48	11.06	3.35
7	10.77	12.34	12.08	11.18	11.59	0.74	11.06	4.79
8	9.94	11.8	12.48	11.11	11.33	1.08	11.07	2.35

Theoretical and experimental velocities are plotted in Figure 7, where it is evident that the outer pipe nozzles, nozzles 1-4, have a lower exiting velocity than the theoretical. On the other hand, the inner pipe nozzles, nozzles 5-8, have a higher exiting velocity than the theoretical value. This is in agreement with observation made regarding mass flow rate.

**Table 9: Velocity per nozzle in m/s**

Nozzle	Test				Average	Theoretical	% Difference
	1	2	3	4			
1	26.98	28.68	26.79	30.34	28.2	29.9	5.69
2	26.8	28.55	28.48	32.02	28.96	29.85	2.98
3	26.71	29.35	29.25	29.79	28.78	29.85	3.58
4	26.53	29.35	30.17	28.86	28.73	29.9	3.91
5	29.05	32.02	30.79	32.58	31.11	30.04	3.56
6	29.23	31.75	30.94	32.21	31.03	30.02	3.36
7	29.23	33.49	32.79	30.34	31.46	30.02	4.8
8	26.98	32.02	33.87	30.16	30.76	30.04	2.4
						Average	3.785

The percent of difference between the experimental and theoretical values were found from:

$$\% \text{ difference} = \frac{|\text{Experimental Value} - \text{Theoretical Value}|}{\text{Theoretical Value}} * 100 \quad (21)$$

The percent difference for mass flow rate and velocity are reported in Tables 1 and 2, respectively. On average, there is a 4% total difference between the average measured values and theoretical predictions. Recall that in the design calculations based on theory, the piping network was idealized during the splits and all minor losses were embedded in one term rather than divided into each energy equation. Therefore, these observed variations could be due to how the minor losses were handled, which were assumed all embedded in one minor loss coefficient.

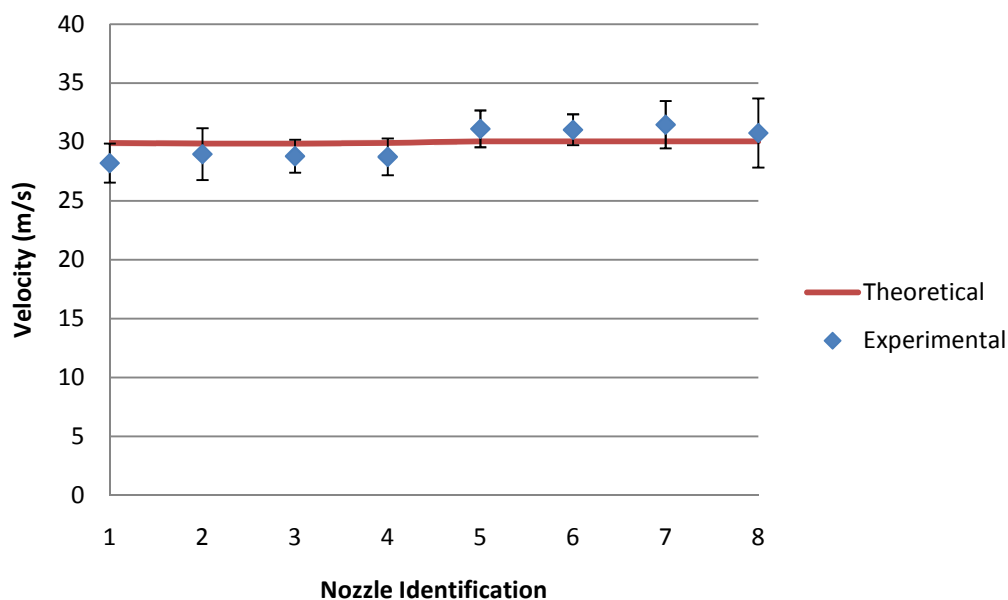


**Figure 7: Average experimental and theoretical outgoing velocity per nozzle (graphical representation of Table 9)**

Due to variations in the mass flow rate per nozzle, a comparison of the total mass flow experimentally measured over a five second period was compared to that expected

theoretically. The results are provided in Table 10 and Figure 8. A difference of about 1 kg is observed which is about 0.25%.

**Table 10: Mass exiting each nozzle and total mass exiting for 5 seconds in kg**

Nozzle	Run				Average	Theoretical
	1	2	3	4		
1	49.7	52.84	49.34	55.89	51.94	55.07
2	49.37	52.59	52.46	58.98	53.35	54.98
3	49.21	54.07	53.88	54.87	53	54.98
4	48.87	54.07	55.58	53.15	52.92	55.07
5	53.51	58.98	56.71	60.01	57.3	55.33
6	53.84	58.49	57	59.32	57.16	55.3
7	53.84	61.68	60.4	55.89	57.95	55.3
8	49.7	58.98	62.38	55.55	56.65	55.33
Sum	408.06	451.69	447.74	453.67	440.29	441.36

From Figure 8 it is hard to see any difference between the experimental and theoretical values. This allows for the conclusion that even though the velocities are not equal through each nozzle, the same amount of water is coming out of the piping network as is predicted from theory. The standard deviation in the experimental velocity, noted in Figure 8, is computed using equation (20).

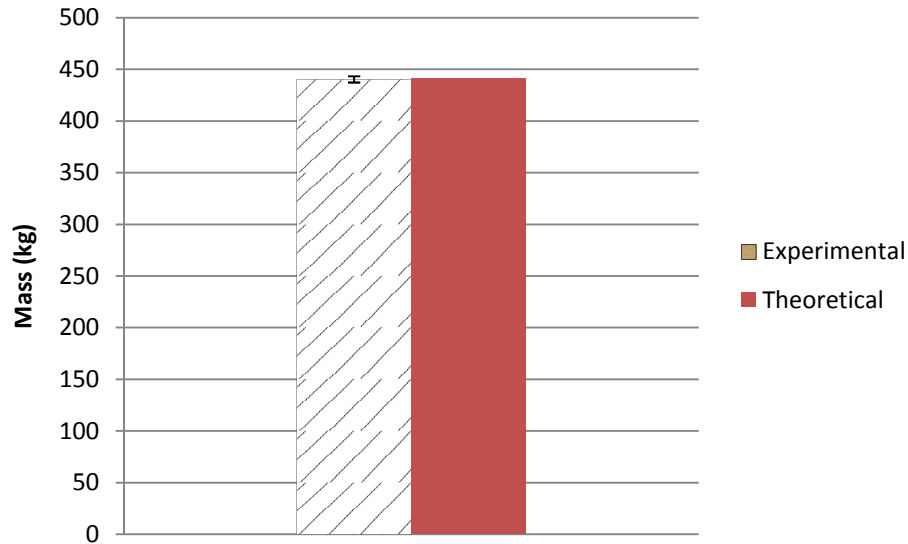


**Figure 8: Total outgoing mass from the piping network for 5 seconds (graphical representation of Table 10)**

From the test results for the SpotCheck, as seen in Table 11, all bottles at all locations passed the food safety test. This is sufficient evidence to show that the cleanliness of the bottle does not depend on the location of the bottle. Since all the bottles are clean, there is a sufficient velocity exiting each nozzle for the bottle washer to be used in a commercial setting.

**Table 11: SpotCheck test results**

Bottle	Location		
	Bottom	Neck	Mouth
1	Pass	Pass	Pass
2	Pass	Pass	Pass
3	Pass	Pass	Pass

## CHAPTER 7: CONCLUSION

The symmetric design of the piping network allows for fairly consistent flow through all the nozzles, with variations between nozzles less than 5.7%. This is acceptable for this application. All the materials used, such as galvanized iron, schedule 40 steel and stainless steel, are compatible with each other and the temperature and chemicals used during the various stages of the dishwashing process.

Through the analyses of mass and energy conservation in the piping network of the retrofit commercial dishwasher, it is found that the total mass that exits the piping network is within  $\pm 0.24\%$  of the predicted value. However, the mass flow rate and velocity out of the nozzles of the piping network varied slightly more, by as much as  $\pm 5.7\%$ , from those predicted. This is attributed to assumptions in flow symmetry and how the minor losses in the junctions were handled. For example, flow through one quarter of the piping network was considered, assuming symmetric flow through the remaining nozzles. Also, rather than computing minor losses at each exit of a component, these losses were combined into a single minor loss at the inlet of the component. Measured mass flow rates and velocities between the eight nozzles varied by as much as 11%. From testing the food safety of the cleaned beer bottles, it is determined that the spray out of each nozzle is enough to effectively clean the beer bottles.

It is proposed that the piping network in the retrofitted commercial dishwasher used for a returnable bottle process can provide a smaller impact on the ozone and solid waste as well as increasing the beauty of the streets and highways. It is an environmentally friendly alternative to throwing away bottles as well as recycling.

**BIBLIOGRAPHY**

- Callister, William D. *Materials Science and Engineering: an Introduction*. New York: John Wiley & Sons, 2007. Print.
- Edahiro, Junko. "Reusable Glass Bottles in Japan." *JFS Newsletter* July 2004. *Mail Magazine*. Web. 10 May 2010.
- Fried, Erwin, and Isaak E. Idelchik. *Flow Resistance: a Design Guide for Engineers*. Washington: Taylor & Francis, 1989. Print.
- Gilson, Christopher C. *Convenience-Package Banning: Economic and Environmental Implications*. Publication. *Springerlink*. Web. 10 May 2010.
- Heim, Samantha, Carolyn Beaudry, and Sean Hunter. *Retrofit Design of a Dishwasher for Reusable Bottles*. Rep. 2010.
- Hygiena. *SpotCheck: Rapid Food Safety Test*. Print.
- Kaminski, Deborah A., and Michael K. Jensen. *Introduction to Thermal and Fluid Engineering*. Hoboken, N.J.: Wiley, 2005.
- Mata, Teresa M., and Carlos A. V. Costa. *Life Cycle Assessment of Different Reuse Percentages for Glass Beer Bottles*. Tech. Landsberg, Germany: Ecomed, 2001.
- Material Safety Data Sheet: Sodium Meta-silicate*. Tech. ScienceLab.com. Web. 17 Jan. 2010.
- SSTC Services Du Premier Ministre. *Characterization of Scuffing on Returnable Bottles*. Rep. *Characterization of Scuffing on Returnable Bottles*. Institut Scientifique Du Verre, Mar. 2000. Web. 5 May 2010.
- White, Frank M. "Head Loss - The Friction Factor." *Fluid Mechanics*. 6th ed. New York: McGraw-Hill, 2008.



## **APPENDICES**

## APPENDIX A: NOZZLE CATALOG

### SOLID-JET *SOLID CONE* NOZZLES

**STANDARD SPRAY ANGLE  
TYPES SF, SM, SSM**

Capacities: .20 to 26 G.P.M.



Type SF  
Female



Type SM  
Male



Type SSM  
Male

Capacity G.P.M. @ 40 PSI	Pipe Size	Catalog No.			Free Passage Size*	CAPACITY IN GALLONS PER MINUTE (At Various Pressures in Pounds Per Square Inch)											SPRAY ANGLES (At Various PSI)											
		Female	Male	Male		3	5	7	10	15	20	30	40	60	80	100	150	7	20	40	80							
		.20	1/8	SF21		SM21	SSM21	.036	—	—	—	—	.12	.14	.17	.20	.25	.28	.35	.40	.49	.57	.63	.78	.39	35°	35°	40°
.40	1/8	SF41	SM41	SSM41	.044	—	.14	.17	.20	.25	.28	.35	.40	.49	.57	.63	.78	.85	.95	1.2	1.6	1.9	2.4	2.9	3.5	4.0	5.0	5.5
.60	1/8	SF61	SM61	SSM61	.044	.16	.21	.25	.30	.37	.42	.52	.60	.74	.85	.95	1.2	1.6	1.9	2.4	2.9	3.5	4.0	5.0	5.5	6.0	7.0	7.5
.80	1/8	SF81	SM81	SSM81	.062	.22	.28	.33	.40	.49	.57	.71	.80	.96	1.1	1.3	1.6	1.9	2.4	2.8	3.2	3.9	4.5	5.5	6.0	7.0	7.5	8.0
1.0	1/8	SF101	SM101	SSM101	.062	.27	.35	.42	.50	.61	.71	.87	1.0	1.2	1.4	1.6	1.9	2.4	2.8	3.2	3.9	4.5	5.5	6.0	7.0	7.5	8.0	8.5
1.0	1/4	SF102	SM102	SSM102	.076	.27	.35	.42	.50	.61	.71	.87	1.0	1.2	1.4	1.6	1.9	2.4	2.8	3.2	3.9	4.5	5.5	6.0	7.0	7.5	8.0	8.5
1.5	1/4	SF152	SM152	SSM152	.086	.41	.53	.63	.75	.92	1.1	1.3	1.5	1.8	2.1	2.4	2.9	3.5	4.0	4.7	5.6	6.3	7.8	8.5	9.5	10.5	11.5	12.5
2.0	1/4	SF202	SM202	SSM202	.086	.55	.71	.84	1.0	1.2	1.4	1.7	2.0	2.4	2.8	3.2	3.9	4.5	5.4	6.3	7.1	8.7	9.5	10.5	11.5	12.5	13.5	14.5
2.5	1/4	SF252	SM252	SSM252	.086	.70	.91	1.1	1.2	1.5	1.8	2.2	2.5	3.1	3.5	3.9	4.8	5.6	6.5	7.5	8.5	9.5	11.5	12.5	13.5	14.5	15.5	16.5
2.0	3/8	SF203	SM203	SSM203	.086	.55	.71	.84	1.0	1.2	1.4	1.7	2.0	2.4	2.8	3.2	3.9	4.5	5.4	6.3	7.1	8.7	9.5	10.5	11.5	12.5	13.5	14.5
2.5	3/8	SF253	SM253	SSM253	.096	.70	.91	1.1	1.2	1.5	1.8	2.2	2.5	3.1	3.5	3.9	4.8	5.6	6.5	7.5	8.5	9.5	11.5	12.5	13.5	14.5	15.5	16.5
3.0	3/8	SF303	SM303	SSM303	.096	.82	1.1	1.3	1.5	1.8	2.1	2.6	3.0	3.7	4.2	4.7	5.8	6.6	7.6	8.6	9.6	11.6	12.6	13.6	14.6	15.6	16.6	17.6
3.5	3/8	SF353	SM353	SSM353	.096	1.0	1.3	1.5	1.1	2.1	2.4	3.0	3.5	4.3	4.9	5.6	6.8	7.7	8.7	9.7	10.7	12.7	13.7	14.7	15.7	16.7	17.7	18.7
4.0	3/8	SF403	SM403	SSM403	.096	1.1	1.4	1.7	2.0	2.4	2.8	3.5	4.0	4.9	5.6	6.3	7.8	8.8	9.8	10.8	11.8	13.8	14.8	15.8	16.8	17.8	18.8	19.8
4.5	3/8	SF453	SM453	SSM453	.096	1.2	1.6	1.9	2.2	2.8	3.2	3.9	4.5	5.4	6.3	7.1	8.7	9.5	10.5	11.5	12.5	13.5	14.5	15.5	16.5	17.5	18.5	19.5
3.5	1/2	SF354	SM354	SSM354	.140	1.0	1.3	1.5	1.7	2.1	2.4	3.0	3.5	4.3	4.9	5.6	6.8	7.7	8.7	9.7	10.7	12.7	13.7	14.7	15.7	16.7	17.7	18.7
4.0	1/2	SF404	SM404	SSM404	.142	1.1	1.4	1.7	2.0	2.4	2.8	3.5	4.0	4.9	5.6	6.3	7.8	8.8	9.8	10.8	11.8	13.8	14.8	15.8	16.8	17.8	18.8	19.8
4.5	1/2	SF454	SM454	SSM454	.142	1.2	1.6	1.9	2.2	2.8	3.2	3.9	4.5	5.4	6.3	7.1	8.7	9.5	10.5	11.5	12.5	13.5	14.5	15.5	16.5	17.5	18.5	19.5
5.0	1/2	SF504	SM504	SSM504	.142	1.4	1.8	2.1	2.4	3.0	3.5	4.3	5.0	6.1	7.1	7.9	9.7	10.7	11.7	12.7	13.7	14.7	15.7	16.7	17.7	18.7	19.7	20.7
5.5	1/2	SF554	SM554	SSM554	.142	1.5	1.9	2.3	2.7	3.4	3.8	4.7	5.5	6.7	7.7	8.6	10.6	11.6	12.6	13.6	14.6	15.6	16.6	17.6	18.6	19.6	20.6	
6.0	1/2	SF604	SM604	SSM604	.142	1.6	2.1	2.5	3.0	3.7	4.2	5.2	6.0	7.3	8.4	9.4	11.6	12.6	13.6	14.6	15.6	16.6	17.6	18.6	19.6	20.6	21.6	
7.0	1/2	SF704	SM704	SSM704	.142	1.9	2.5	2.9	3.5	4.3	4.9	6.1	7.0	8.6	9.9	11.1	13.6	14.6	15.6	16.6	17.6	18.6	19.6	20.6	21.6	22.6	23.6	24.6
8.0	1/2	SF804	SM804	SSM804	.142	2.2	2.8	3.3	4.0	4.9	5.7	6.9	8.0	9.8	11.2	12.7	15.5	16.5	17.5	18.5	19.5	20.5	21.5	22.5	23.5	24.5	25.5	26.5
6.0	3/4	SF606	SM606	SSM606	.187	1.6	2.1	2.5	3.0	3.7	4.2	5.2	6.0	7.3	8.4	9.4	11.6	12.6	13.6	14.6	15.6	16.6	17.6	18.6	19.6	20.6	21.6	22.6
7.0	3/4	SF706	SM706	SSM706	.190	1.9	2.5	2.9	3.5	4.3	4.9	6.1	7.0	8.6	9.9	11.1	13.6	14.6	15.6	16.6	17.6	18.6	19.6	20.6	21.6	22.6	23.6	24.6
8.0	3/4	SF806	SM806	SSM806	.190	2.2	2.8	3.3	4.0	4.9	5.7	6.9	8.0	9.8	11.2	12.7	15.5	16.5	17.5	18.5	19.5	20.5	21.5	22.5	23.5	24.5	25.5	26.5
9.0	3/4	SF906	SM906	SSM906	.190	2.4	3.2	3.8	4.5	5.6	6.3	7.8	9.0	11.0	12.6	14.1	17.4	18.4	19.4	20.4	21.4	22.4	23.4	24.4	25.4	26.4	27.4	28.4
10.0	3/4	SF1006	SM1006	SSM1006	.190	2.7	3.6	4.2	4.9	6.1	7.1	8.7	10.0	12.3	14.2	15.8	19.4	20.4	21.4	22.4	23.4	24.4	25.4	26.4	27.4	28.4	29.4	30.4
12.0	3/4	SF1206	SM1206	SSM1206	.190	3.3	4.3	5.0	6.0	7.3	8.5	10.4	12.0	14.7	17.0	19.0	23.2	24.2	25.2	26.2	27.2	28.2	29.2	30.2	31.2	32.2	33.2	34.2
14.0	3/4	SF1406	SM1406	SSM1406	.190	3.8	5.0	5.8	7.0	8.5	9.9	12.1	14.0	17.1	19.8	22.1	27.0	28.0	29.0	30.0	31.0	32.0	33.0	34.0	35.0	36.0	37.0	38.0
16.0	3/4	SF1606	SM1606	SSM1606	.190	4.4	5.7	6.7	8.0	9.8	11.3	13.6	16.0	19.6	22.6	25.3	31.0	32.0	33.0	34.0	35.0	36.0	37.0	38.0	39.0	40.0	41.0	42.0
10.0	1	SF1008	SM1008	SSM1008	.234	2.7	3.6	4.2	5.0	6.1	7.1	8.7	10.0	12.3	14.2	15.8	19.4	20.4	21.4	22.4	23.4	24.4	25.4	26.4	27.4	28.4	29.4	30.4
12.0	1	SF1208	SM1208	SSM1208	.244	3.3	4.3	5.0	6.0	7.3	8.5	10.4	12.0	14.7	17.0	19.0	23.2	24.2	25.2	26.2	27.2	28.2	29.2	30.2	31.2	32.2	33.2	34.2
14.0	1	SF1408	SM1408	SSM1408	.244	3.8	5.0	5.8	7.0	8.5	9.9	12.1	14.0	17.1	19.8	22.1	27.0	28.0	29.0	30.0	31.0	32.0	33.0	34.0	35.0	36.0	37.0	38.0
16.0	1	SF1608	SM1608	SSM1608	.244	4.4	5.7	6.7	8.0	9.8	11.3	13.8	16.0	19.6	22.6	25.3	31.0	32.0	33.0	34.0	35.0	36.0	37.0	38.0	39.0	40.0	41.0	42.0
18.0	1	SF1808	SM1808	SSM1808	.244	4.9	6.4	7.5	9.0	11.0	12.7	15.6	18.0	22.0	25.4	28.4	34.8	35.8	36.8	37.8	38.8	39.8	40.8	41.8	42.8	43.8	44.8	45.8
20.0	1	SF2008	SM2008	SSM2008	.244	5.5	7.1	8.4	10.0	12.2	14.1	17.3	20.0	24.5	28.2	31.6	38.8	39.8	40.8	41.8	42.8	43.8	44.8	45.8	46.8	47.8	48.8	49.8
24.0	1	SF2408	SM2408	SSM2408	.244	6.6	8.5	10.1	12.0	14.7	17.0	20.8	24.0	29.4	34.0	38.0	46.4	47.4	48.4	49.4	50.4	51.4	52.4	53.4	54.4	55.4	56.4	57.4
26.0	1	SF2608	SM2608	SSM2608	.244	7.0	9.3	11.0	13.0	15.8	18.4	22.4	26.0	32.0	36.7	41.1	50.5	51.5	52.5	53.5	54.5	55.5	56.5	57.5	58.5	59.5	60.5	61.5

\*Determines maximum foreign particle size that will flow through nozzle without clogging.

### SOLID-JET TYPES SF, SM, SSM DIMENSIONS AND WEIGHTS

Type SF				Type SM				Type SSM			
FEMALE CONNECTION				MALE CONNECTION				MALE CONNECTION			
Pipe Size	Net Weight	A	B	Pipe Size	Net Weight	A	B	Pipe Size	Net Weight	A	B
1/8	3/4 oz.	9/16	1 1/16	1/8	3/4 oz.	9/16	1 1/8	1/8	1/2 oz.	1/2	5/8
1/4	1 1/4 oz.	1 1/16	1 3/8	1/4	1 1/2 oz.	1 1/					

## APPENDIX B: PIPING NETWORK PART SUMMARY

**Table B1: Material and quantity of the piping network parts**

Quantity	Name	Material	Source	Manufacturer's Part Number
1	3/4" x 1" x 3/4" Reducing Tee	Galvanized Iron	McMaster- Carr	4638K177
2	3/4" Pipe Cross	Galvanized Iron	McMaster- Carr	4638K424
2	3/4" Nipple 1 1/2" Length	Galvanized Sch. 40 Steel	McMaster- Carr	4549K592
2	1/2" x 3/4" x 1/2" Reducing Tee	Galvanized Iron	McMaster- Carr	4638K187
2	3/4" Nipple 3" Length	Galvanized Sch. 40 Steel	McMaster- Carr	4549K595
8	1/2" x 1/4" x 1/2" Reducing Tee	Galvanized Iron	McMaster- Carr	4638K175
8	1/2" Nipple 2 1/2" Length	Galvanized Sch. 40 Steel	McMaster- Carr	4549K574
8	1/2" 90 Deg Elbow	Galvanized Iron	McMaster- Carr	4638K193
4	1/2" Nipple 1 1/2" Length	Galvanized Sch. 40 Steel	McMaster- Carr	4549K573
16	1/4" Nozzle	Steel	Steinen	SSM202
4	1/2" Nipple 2" Length	Galvanized Sch. 40 Steel	McMaster- Carr	4549K572

## APPENDIX C: NOMENCLATURE

**Table C1: Nomenclature used throughout equations**

Variable	Definition
$d$	Diameter [m]
$L$	Length [m]
$\rho$	Density [ $\text{kg}/\text{m}^3$ ]
$\mu$	Viscosity [ $\text{N}\cdot\text{s}/\text{m}^2$ ]
$m$	Mass [kg]
$A$	Area [ $\text{m}^2$ ]
$v$	Velocity [m/s]
$\dot{m}$	Mass flow rate [kg/s]
$P$	Pressure [kPa]
$g$	Acceleration due to gravity [ $\text{m}/\text{s}^2$ ]
$\gamma$	Specific gravity [ $\text{kg}/\text{m}^2\cdot\text{s}^2$ ]
$z$	Elevation [m]
$h_f$	Frictional head loss [m]
$f$	Friction factor
$Re$	Reynolds number
$\varepsilon$	Roughness value [m]
$h_m$	Minor head loss [m]
$\zeta$	Minor loss coefficient
$\dot{V}$	Volumetric flow rate [ $\text{m}^3/\text{s}$ ]
$t$	Time [s]
$\sigma$	Standard deviation
$N$	Number of total runs
$x$	Value for each run
$\bar{x}$	Average value
$u_t$	Uncertainty of time [s]
$u_m$	Uncertainty of mass [kg]

## APPENDIX D: PIPING NETWORK CALCULATIONS

$g=9.8$   
 $Q_{n\_english}=1.7$   
 $Q_n=(Q_{n\_english}*.003785/60)$   
 $d_{nozzle}=.086*.0254$   
 $v_{n\_exit}=Q_n/((d_{nozzle}/2)^2*3.14159)$   
 $P_{loss\_nozzle}=30*6894.76$   
 $\rho=983$   
 $\mu=0.000467$   
 $K_{nozzle}=P_{loss\_nozzle}/\rho*v_{n\_exit}^2$   
 $P_{in}=35*6894.76$   
 $d_{in}=0.0254$   
 $d_1=.75*0.0254$   
 $d_2=d_1$   
 $d_3=.5*0.0254$   
 $d_5=d_3$   
 $d_7=d_3$   
 $d_9=d_3$   
 $e_{ir}=0.00026$

$Re_{in}=v_{in}*d_{in}*\rho/\mu$   
 $Re_1=v_1*d_1*\rho/\mu$   
 $Re_2=v_2*d_1*\rho/\mu$   
 $Re_3=(v_3+v_5)*d_3*\rho/\mu$   
 $Re_5=v_5*d_5*\rho/\mu$   
 $Re_7=(v_7+v_9)*d_7*\rho/\mu$   
 $Re_9=v_9*d_9*\rho/\mu$

$f_{in}=(1/(-1.8*\text{LOG}_{10}(((e_{ir}/d_{in})/3.7)^{1.11}+6.9/Re_{in})))^2$   
 $f_1=(1/(-1.8*\text{LOG}_{10}(((e_{ir}/d_1)/3.7)^{1.11}+6.9/Re_1)))^2$   
 $f_2=(1/(-1.8*\text{LOG}_{10}(((e_{ir}/d_2)/3.7)^{1.11}+6.9/Re_2)))^2$   
 $f_3=(1/(-1.8*\text{LOG}_{10}(((e_{ir}/d_3)/3.7)^{1.11}+6.9/Re_3)))^2$   
 $f_5=(1/(-1.8*\text{LOG}_{10}(((e_{ir}/d_5)/3.7)^{1.11}+6.9/Re_5)))^2$   
 $f_7=(1/(-1.8*\text{LOG}_{10}(((e_{ir}/d_7)/3.7)^{1.11}+6.9/Re_7)))^2$   
 $f_9=(1/(-1.8*\text{LOG}_{10}(((e_{ir}/d_9)/3.7)^{1.11}+6.9/Re_9)))^2$

$L_1=2.5*0.0254$   
 $L_2=3*0.0254$   
 $L_3=2.5*0.0254$   
 $L_5=3*0.0254$   
 $L_7=L_3$   
 $L_9=L_3$   
 $z_{in}=0.0254$

$f_{min}=z_{in}$   
 $f_{m1}=2*v_1^2/(2*g)$

$$\begin{aligned}
f_{m3} &= 2*(v_3+v_5)^2/(2*g) \\
f_{m5} &= v_5^2/(2*g) \\
f_{m7} &= 2*(v_7+v_9)^2/(2*g) \\
f_{m9} &= v_9^2/(2*g) \\
f_{m2} &= 2*v_2^2/(2*g) \\
f_{n4} &= K_{nozzle}*v_{n_4}^2/(2*g)+2*v_3^2/(2*g) \\
f_{n6} &= K_{nozzle}*v_{n_6}^2/(2*g) \\
f_{n8} &= K_{nozzle}*v_{n_8}^2/(2*g)+2*v_7^2/(2*g) \\
f_{n10} &= K_{nozzle}*v_{n_{10}}^2/(2*g)
\end{aligned}$$

$$\begin{aligned}
P_{loss\_in} &= f_{min}+f_{in}*z_{in}/d_{in}*v_{in}^2/(2*g) \\
P_{loss\_1} &= f_1*L_1/d_1*v_1^2/(2*g)+f_{m1} \\
P_{loss\_3} &= f_3*L_3/d_3*(v_3+v_5)^2/(2*g)+f_{m3} \\
P_{loss\_5} &= f_5*L_5/d_5*v_5^2/(2*g)+f_{m5} \\
P_{loss\_2} &= f_2*L_2/d_2*v_2^2/(2*g)+f_{m2} \\
P_{loss\_7} &= f_7*L_7/d_7*(v_7+v_9)^2/(2*g)+f_{m7} \\
P_{loss\_9} &= f_9*L_9/d_9*v_9^2/(2*g)+f_{m9} \\
P_{in}/(\rho*g) &= P_{loss\_in}+P_{loss\_1}+P_{loss\_3}+f_{n4} \\
P_{in}/(\rho*g) &= P_{loss\_in}+P_{loss\_1}+P_{loss\_3}+P_{loss\_5}+f_{n6} \\
P_{in}/(\rho*g) &= P_{loss\_in}+P_{loss\_1}+P_{loss\_2}+P_{loss\_7}+f_{n8} \\
P_{in}/(\rho*g) &= P_{loss\_in}+P_{loss\_1}+P_{loss\_2}+P_{loss\_7}+f_{n10} \\
v_{in}*(d_{in}/2)^2*\pi &= 2*v_1*(d_1/2)^2*\pi \\
\rho*(d_3/2)^2*\pi*v_3 &= \rho*(d_{nozzle}/2)^2*\pi*v_{n_4} \\
\rho*(d_3/2)^2*\pi*v_5 &= \rho*(d_{nozzle}/2)^2*\pi*v_{n_6} \\
\rho*(d_3/2)^2*\pi*v_7 &= \rho*(d_{nozzle}/2)^2*\pi*v_{n_8} \\
\rho*(d_3/2)^2*\pi*v_9 &= \rho*(d_{nozzle}/2)^2*\pi*v_{n_{10}} \\
v_2*(d_1/2)^2*\pi &= 2*(v_7+v_9)*(d_3/2)^2*\pi
\end{aligned}$$

$$\begin{aligned}
L_{u_1} &= 10.5*0.0254 \\
L_{u_2} &= 11*0.0254 \\
L_{u_3} &= 22*0.0254 \\
L_{u_4} &= 13.5*0.0254 \\
d_{u_1} &= 0.96*0.0254 \\
d_{u_2} &= 0.6*0.0254 \\
d_{u_n} &= .003969 \\
Re_u &= v_u*\rho*d_{u_1}/\mu \\
f_u &= (.79*LN(Re_u)-1.64)^{-2} \\
P_{u\_loss} &= f_u*L_{u_1}/d_{u_1}*v_u^2/(2*g)+0.72*v_u^2/(2*g)+f_u*L_{u_2}/d_{u_1}*v_u^2/(2*g)+f_u*L_{u_3}/d_{u_1}*v_u^2/(2*g)+f_u*L_{u_4}/d_{u_1}*v_u^2/(2*g)+3*1.5*v_u^2/(2*g)+L_{u_3} \\
10*v_{u_n}*(d_{u_2}/2)^2*\pi &= v_u*(d_{u_1}/2)^2*\pi \\
v_{u_n}*(d_{u_2}/2)^2 &= v_{u\_exit}*(d_{u_n}/2)^2 \\
Q_{u\_nozzle} &= 2.6*0.003785/60 \\
v_{u\_nozzle} &= Q_{u\_nozzle}/((d_{u_n}/2)^2*\pi) \\
K_{u\_nozzle} &= P_{loss\_nozzle}/\rho*v_{u\_nozzle}^2 \\
P_{in}/(\rho*g) &= P_{u\_loss}+(K_{u\_nozzle}*v_{u\_exit}^2/(2*g)+1.45*v_{u_n}^2/(2*g))
\end{aligned}$$

## APPENDIX E: VARIABLE VALUES

**Table E1: Reynolds numbers for individual pipe sections**

Frictional Head Loss Variable	Reynolds Number
$h_{f1}$	117000
$h_{f2}$	63400
$h_{f3}$	47500
$h_{f5}$	23800
$h_{f7}$	47500
$h_{f9}$	23800

**Table E2: Friction factor values for individual pipe sections**

Piping Section	Friction Factor, $f$
1	0.0388
2	0.0392
3	0.0394
5	0.0405
7	0.0394
9	0.0405

**Table E3: Frictional head loss values for individual pipe sections**

Piping Section	Frictional Head Loss
1	0.933
2	0.020
3	0.266
5	0.091
7	0.266
9	0.091

**Table E4: Minor head loss values for individual pipe sections**

Piping Section	Minor Head Loss
$h_{mA}$	0.025
$h_{mB}$	0.876
$h_{mC}$	0.322
$h_{mD}$	23.7
$h_{mE}$	0.040
$h_{mF}$	23.7
$h_{mG}$	0.252
$h_{mH}$	0.320
$h_{mI}$	23.5
$h_{mJ}$	0.040
$h_{mK}$	23.5

